V-Proportion: A Method Based on the Voronoi Diagram to Study Spatial Relations in Neuronal Mosaics of the Retina

Oscar Martinez Mozos[a,*], Jose A. Bolea[b], Jose M. Ferrandez[c], Peter K. Ahnelt[d], Eduardo Fernandez[b]

[a]*Dept. of Computer Science and System Engineering, University of Zaragoza, Spain*
[b]*Bioengineering Institute, Miguel Hernandez University, Spain*
[c]*Dept. of Electronics and Comp. Technology, Technical University of Cartagena, Spain*
[d]*Dept. of Physiology, Medical University of Vienna, Austria*

Abstract

The visual system plays a predominant role in the human perception. Although all components of the eye are important to perceive visual information, the retina is a fundamental part of the visual system. In this work we study the spatial relations between neuronal mosaics in the retina. These relations have shown its importance to investigate possible constraints or connectivities between different spatially colocalized populations of neurons, and to explain how visual information spreads along the layers before being sent to the brain. We introduce the V-Proportion, a method based on the Voronoi diagram to study possible spatial interactions between two neuronal mosaics. Results in simulations as well as in real data demonstrate the effectiveness of this method to detect spatial relations between neurons in different layers.

Keywords: Voronoi Diagram, Spatial Relations, Neuronal Mosaics, Retina

1. Introduction

In the last decades, the development of technological advances has been largely inspired by nature and specially by biological systems. This is even more relevant in the fields of artificial intelligence and cognition, where computer scientists are often looking for models that mimic the characteristics of perception and information processing performed by the human brain and by the different sensory systems attached to it.

One of the most important sensory systems in humans is the visual system. In the human brain, 30% of the sensory neurons belong to this system [1]. This fact corroborates the predominant role of the visual sense in the human perception. Although all components of the eye are important to perceive visual information, the retina is a fundamental part of the visual system. The retina is basically a piece of brain tissue that gets direct stimulations from the outside world's lights and images [2]. A relatively easy access to the retina, together with the possibility of studying the information processing in an intact portion of the nervous system make this part of the eye a unique model to study the nervous system in general [3] and the visual system in particular [4].

There exist several attempts to develop bio-inspired artificial retinas with the purpose of replacing or partially recovering damaged functionalities in perception [5, 6]. Moreover, retinal-inspired models have been used to improve the vision system in robots [7, 8]. However, the complete information process inside the retina is not fully understood yet. A central challenge is therefore to understand how the retina is designed to solve the image processing task.

The retina is organized into layers formed by many local neuronal circuits which work in parallel with each other to asses the different aspects of an image. In each layer, neurons of the same type are spatially distributed into regular or irregular patterns known as *retinal mosaics*. The neurons often have dendrites that extend in a competitive manner reducing the overlap of their dendritic fields and resulting in a tessellation across the retina [9, 10]. As a result, an assembly of efficiently-

*Corresponding author at: Dept. of Computer Science and System Engineering (DIIS), University of Zaragoza. Edificio Ada Byron, C/Maria de Luna, 1. 50018 Zaragoza. Spain. Phone: +34 97 676 2472. Fax: +34 976 761 914.

Email addresses: ommozos@unizar.es (Oscar Martinez Mozos), joseangel.bolea@educa.madrid.org (Jose A. Bolea), jm.ferrandez@upct.es (Jose M. Ferrandez), peter.ahnelt@univie.ac.at (Peter K. Ahnelt), e.fernandez@umh.es (Eduardo Fernandez)

connected functional circuits between the mosaics of different neuronal subtypes is created. The study of the spatial relations between these mosaics is highly relevant to understand how the visual information spreads along the different layers, and how it is finally processed before being sent to the brain.

The study of the spatial relations between neural populations has also shown its importance to investigate possible constrains or connectivities between different cell types. A positive spatial dependency between two different populations of neurons may be an indicator of some connection patterns between them [11, 12, 13, 14]. The spatial information is moreover helpful to study dependencies during development [15].

This paper introduces a method to study spatial relations between two neuronal mosaics in the retina. The key idea of this work is to calculate the Voronoi diagram in one of the populations, and then study the distribution of neurons from the second population inside the polygons of the diagram. Using polygonal areas around neuronal cells is a realistic approximation, since neurons present different irregularities in their structure [16].

The remaining part of the paper is organized as follows. After introducing some related work in Sect. 2, we describe the Voronoi diagram in Sect. 3. The V-Proportion measurement is presented in Sect. 4. We validate this method with simulated populations in Sect. 5. Several real neuronal mosaics from the retina are analyzed in Sect. 6. Finally, we conclude in Sect. 7.

2. Related Work

Different methods to study spatial relations between two cell populations have been proposed in the past. An extension of the density recovery profile (DRP) [17] for two populations is used in the work by Kouyama and Marshak [18] to study interdependences between two types of S-cone cells. This extension is called cross-correlational density recovery profile (cDRP). Opposite to the conventional DRP, which is based on autocorrelations of the same population, the cDRP uses one of the populations as reference and calculates the correlation of the second population.

The different DRP methods are based on circular domains around the reference cells. In contrast to this technique, the V-Proportion measurement is based on polygonal domains around the cells, which generally provide more adequate spatial approximations of dendritic fields than circles [14]. However, since our Voronoi procedure is based solely on the locations of cell bodies and does not produce concave corners, it may also fail for cells with extreme dendritic domains.

Another measurement used to study spatial dependencies is the K-function [19], which uses second order analysis of stationary point processes. The K-function is used by Diggle [20] to analyze the spatial relation between on- and off-cells in the retina. A multivariate counterpart of the J-function [21] is introduced by Lieshout and Baddeley [22] to study possible interdependences between two population of points. The authors applied this metric to study spatial dependencies of beta cells in the cat retina [22].

K-nearest neighbor histograms have been also applied to study possible spatial correlations between neuronal mosaics. For example, Wässle et al. [23] apply this method to study Beta cells in the cat retina.

In the work by Diggle et al. [24], the authors use Monte Carlo methods for conducting likelihood-based analysis of point process models in neuronal data. In particular, they fit a bivariate pairwise interaction model in point data corresponding to retinal amacrine cells.

In the previous methods, only the coordinates of the center of the cells are used. Our V-Proportion method, however, applies a domain around the reference cells to study possible spatial relations between the different populations. This domains adapt better to the dendritic fields of neurons.

Finally, Ahnelt et al. [14] apply a first version of the V-Proportion to analyze interactions between irregular S-cone mosaics and axonless horizontal cells. In comparison to [14], this paper presents several improvements. First, we solve the edge problem by ignoring points lying on open Voronoi polygons. This approximation reduces the number of points used in the statistics, however it increases the confidence of the final results. Second, in this paper we introduce a method to determine the level of spatial correlation between two populations. In addition, we apply the V-Proportion to real populations whose possible spatial correlations have not been studied before.

3. The Voronoi Diagram

The Voronoi diagram is one of the most useful geometrical constructions to study point patterns, since it provides all the information needed to study proximity relations between points [25].

A Voronoi diagram can be defined as follows. Let $S = \{s_1, s_2, \ldots, s_n\}$ be a limited set of points in the two-dimensional Euclidean plane. These points are also called *Voronoi sites*. Now each site s_i is assigned the rest of points in the plane $p \notin S$ which are nearest to it

$$V(s_i) = \{p \mid d(p, s_i) \leq d(p, s_j);\ p \notin S,\ \forall s_j \neq s_i\} \quad (1)$$

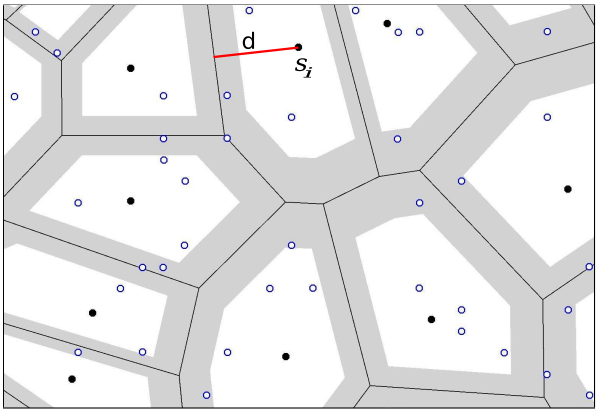

Figure 1: Part of a Voronoi diagram (black lines) for a set of sites (filled circles). Bands around the edges of the Voronoi diagram are shown in grey. In this particular case $\delta = 0.29$, indicating the 29% of the distance d between a Voronoi edge and its closest site s_i. The P population is shown in open circles.

with $d(.,.)$ representing the Euclidean distance function.

This process creates a tessellation of the plane into (sometimes unbounded) convex polytopes, also called *Voronoi polygons*. Let $V(s_i)$ be the Voronoi polygon corresponding to the site s_i, then all the points inside this polygon are at least as close to s_i as to any other site s_j.

The edges of the Voronoi polygons form the Voronoi diagram $V(S)$ of the sites S. Note that a point lying on one edge of the Voronoi diagram has two nearest neighbors sites, and each vertex has at least three. An example of a Voronoi diagram is shown in Fig. 1.

4. The V-Proportion Measurement

The main idea of this work is to study spatial interdependences between two neuronal populations. Each neuron is represented by a point in the two-dimensional Euclidean plane. Usually these points correspond to the cell bodies of the neurons.

Our method consists of two main steps. In the first one, we select a population as the set of sites from which we calculate the Voronoi diagram. This diagram is extended with a set of bands around the edges of the Voronoi polygons. In the second step, the remaining population is superimposed on the Voronoi diagram and a set of statistics are calculated, which represent the spatial relations between both populations.

First, the Voronoi diagram of the sites S is calculated using the criterion in (1). After obtaining the Voronoi diagram we establish a set of bands around the edges of the resulting Voronoi polygons. These bands are shown as grey areas in Fig. 1. The width of each band is not fixed but is proportional to the distance between a given edge and its closest site. This proportion is represented by the parameter δ with $0 < \delta < 1$. We then superimpose the set of points P, which corresponds to the second population of cells, on the extended Voronoi diagram containing the bands.

The basic idea behind this configuration is the following. If both populations S and P are spatially independent, then the occurrence of a site point should not alter the probability of the occurrence of P points, and the average density of P points should be the same inside and outside the bands. However, it could happen that P points show either a positive or negative spatial correlation with the sites. If the sites inhibit the P points, then the latter will appear near the edges of the Voronoi diagram, and the number of P points inside the bands will be significantly higher than expected. On the contrary, when the number of P points inside the band is decreased, it will mean that the sites are positively correlated to them.

Using the previous concepts, we define the V-Proportion value as the relation between the number of points inside the bands and the total number of points

$$\text{V-Proportion} = \frac{|P_B|}{|P|}, \tag{2}$$

with the set $P_B \subseteq P$ defined as

$$P_B = \{p_j \in P \mid d(p_j, e_j) \leq \delta \cdot d(s_i, e_j), \text{if } p_j \in V(s_i)\}, \tag{3}$$

where e_j is the nearest $V(s_i)$ edge to the point p_j. The set P_B thus represents the subset of P points lying inside the bands of the extended Voronoi diagram. The V-Proportion value varies depending on the width of the bands, which is indicated by the parameter δ.

The interpretation of the V-Proportion measurement is as follows. If the V-Proportion is higher than expected, that would suggest a negative correlation between S and P. On the contrary, if the measured V-Proportion is smaller than expected, that would indicate a positive correlation.

An example of this process is shown in Fig. 1. This figure shows two populations of points representing two different types of cells. Each cell is represented by the 2D coordinates of its center. The point population depicted in filled circles is used as sites for the Voronoi diagram. The resulting edges of the Voronoi diagram are shown in black lines. Following the previous approach, the edges were extended with bands whose sizes are dependent on the distance of each edge in the direction to its closest site (grey bands). In this particular case

$\delta = 0.29$, indicating that the band width is 29% of the distance d to its closest site s_i. In a next step, the second point population P (marked as open circles) was superimposed to the obtained geometrical construction.

To test the significance of the V-Proportion, we use a Monte Carlo test procedure. This involves generating a set of two random and independent patterns, each with the same number of points as the two empirical populations S and P, and in a study area identical to that of these patterns. We repeat the generation T times for different values of δ, and then the mean and the standard deviation of each simulated V-Proportion are calculated. The resulting plot is compared with the V-Proportion obtained with the two real S and P populations. Whenever the real V-Proportion raises above the random equivalent simulation, then we can assume a negative interaction between populations, that is, S inhibits P. If the real V-Proportion is below the simulated one, then a clustering process occurs in which S points attract P points. If the real V-Proportion is close to the simulated one, we can not assume any significant spatial interaction between the two populations.

Finally, an important problem when working with point populations is the edge effect. Typically, the observation of the two point patterns is restricted to a regular sampling window, while usually the patterns extend beyond it. Furthermore, the Voronoi polygons on the boundary of the window are open because they have no neighboring points in those directions as shown in Fig. 2. This edge effect affects the sense of bands in the Voronoi polygons adjacent to the edges. In our case, we solve this problem by removing the Voronoi polygons intersecting the edges of the sampling area (open polygons). Similar approaches have been applied in other works for studying cell mosaics [26, 27]. Although this heuristic reduces the total number of points used for the study, we think the results represent the spatial relations in a more reliable manner.

5. Validation of the V-Proportion Measurement

In this section we present a validation of the proposed V-Proportion measurement. We analyze several pairs of simulated populations following different spatial relations. In particular, we simulate pairs of populations showing a positive correlation, a negative correlation, and neither positive nor negative correlation. We then calculate the V-Proportion for each of the simulated pair of populations. The results indicate that we can clearly detect the three previous behaviors using the V-Proportion measurement. We finally present some guidelines to determine the level of positive/negative correlation using the V-Proportion plot.

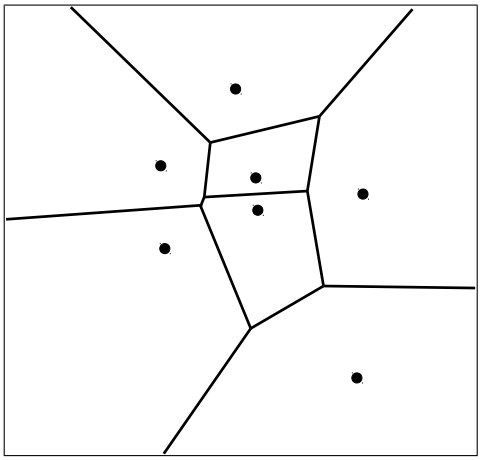

Figure 2: Voronoi diagram (black lines) for a set of sites (filled circles). The polygons close to the borders of the sampling window remain open since there are no neighboring points in those directions.

5.1. Detection of a Positive Correlation

The first behavior we want to detect is a positive correlation between two point populations. A positive correlation means that the points in one population tend to form clusters around the points of the other population. To simulate this behavior we apply the Poisson cluster process introduced in [28, 29]. We first generate the site points following a bi-dimensional Poisson process. For each site, a set of offspring points is generated (P population). The positions of the offspring points relative to their corresponding sites are independent and identically distributed according to a bi-dimensional normal distribution. More details on the implementation can be found in [30].

Different pairs of populations were generated following this approach. All pairs contained the same number of sites and P points: 50 and 300 respectively. The populations were contained in an image area of 300×300 pixels. For each pair of populations, a different variance σ^2 was used for the bi-dimensional normal distribution of the offspring points. Example simulations together with their corresponding V-Proportion plots are shown in Fig. 3 and Fig. 4. The clusters in Fig. 3(a) were simulated with a variance of $\sigma^2 = 25$ (in pixel units). In this case the clustering was detected within a confidence interval of 95% (Fig. 3(b)). The clusters in Fig. 4(a) have a variance of $\sigma^2 = 100$. This clustering was still detected within a confidence interval of 95% using the V-Proportion measurement (Fig. 4(b)).

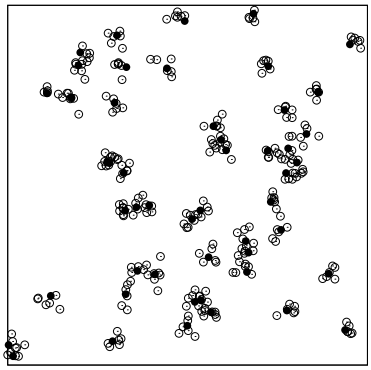

(a) $\sigma^2 = 25$

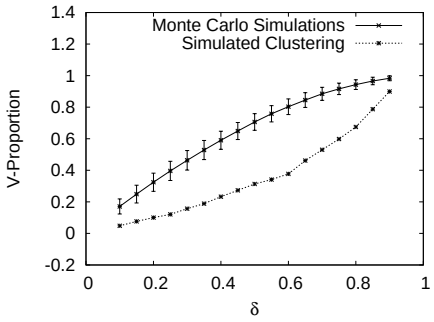

(b) V-Proportion

Figure 3: (a) A Poisson cluster with $\sigma^2 = 25$ in pixel units. The area of the original image is 300×300 pixels. Sites are shown as filled circles, whereas *P* points are depicted as open circles. (b) Plot of the V-Proportion with error bars drawn at the 95% confidence interval. The clustering is clearly detected by the V-Proportion.

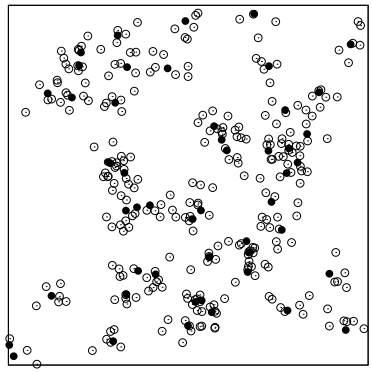

(a) $\sigma^2 = 100$

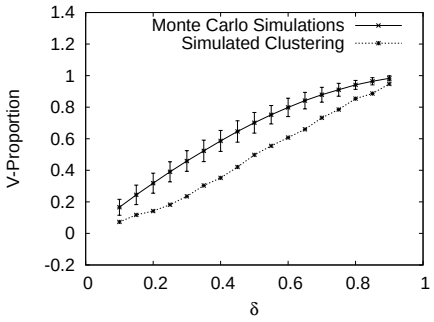

(b) V-Proportion

Figure 4: (a) A Poisson cluster with $\sigma^2 = 100$ in pixel units. The area of the original image is 300×300 pixels. Sites are shown as filled circles, whereas *P* points are depicted as open circles. (b) Plot of the V-Proportion with error bars drawn at the 95% confidence interval. The clustering is detected within a confidence interval of 95%.

5.2. Detection of a Negative Correlation

The second behavior we want to detect is a negative correlation between two point populations. A negative correlation means that points from one population tend to be far away from the points in the other population. A way to simulate this kind of behavior consists of generating offspring points that can not be closer to any site point less than a certain distance. To generate pairs of populations with negative correlations we followed the method presented in [31]. This approach generates a site population in which the sites are separated each other by a certain distance. A second population is generated whose points are not allowed to be closer to a site point by a distance smaller than a certain threshold. Fig. 5(a) presents a pair of populations following the previous criteria. In this case the sites (filled circles) have a minimum distance of 60-80 pixels between them. The *P* points (open circles) are generated with a minimum distance of 70-80 pixels to the closest site. The V-Proportion plot in Fig. 5(b) clearly indicates a negative correlation between both populations within the 95% confidence interval.

5.3. Lack of Spatial Correlation

The third behavior we are interested in is the lack of spatial correlation between two populations. In our case this means that the populations does not present neither positive nor negative correlation. To simulate this behavior we randomly generate two populations in a certain area, each population following a bi-dimensional Poisson distribution. Example of such simulation can be shown in Fig. 6(a). In this case we generated 50 sites and 300 *P* points in an image area of 300×300 pixels. The resulting V-Proportion plot is presented in Fig. 6(b). The real V-Proportion maintains inside the confidence interval of the Monte Carlo simulated populations which indicates no spatial correlation at all.

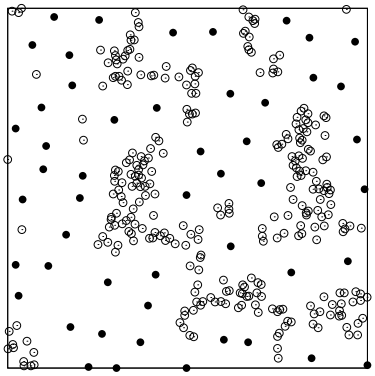

(a) Negative Correlation

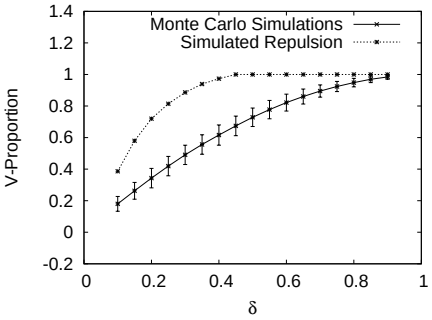

(b) V-Proportion

Figure 5: (a) The image shows two populations with a negative correlation. Sites are shown in filled circles while *P* points are depicted as open circles. (b) The V-Proportion plot suggests a negative correlation. Error bars are drawn at the 95% confidence interval.

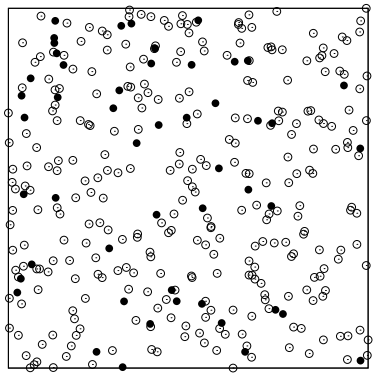

(a) Random Populations

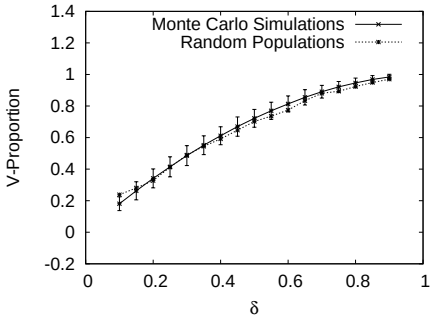

(b) V-Proportion

Figure 6: (a) The image shows two random populations. Sites are shown in filled circles while *P* points are depicted as open circles. (b) According to the V-Proportion plot there is no evidence of a positive or negative correlation. Error bars are drawn at the 95% confidence interval.

5.4. Determining the Level of Correlation

As shown in the previous experiments, the V-Proportion is able to detect positive or negative correlations using different confidence intervals. Once the level of confidence is set, the V-Proportion of the population to be analyzed is compared with the simulated data. We can interpret the resulting plot is as follows. Whenever the V-Proportion of the analyzed population lies above (or below) the confidence intervals of the simulated population for any band width δ, we can assume a negative (or positive) correlation.

A way to measure the level of correlation is to calculate the area between the V-Proportion curves of the real patterns and the random simulations. Bigger areas would imply higher levels of correlation. An example is shown in the plot of Fig. 7(a). This plot corresponds to the negative correlation example of Fig. 5. The area between the real V-Proportion and the simulated one is depicted in grey color. Alternatively, it could be interesting to concentrate on some specific band width subinterval (Fig. 7(b)).

Using this method we can find the band width subinterval, which is directly related to the subinterval of distances to the central body of the neurons, that gives the best significance for the probability of containing the major part of the second population in the mosaic.

6. Experiments with Real Populations

In this section we analyze different pairs of neuronal mosaics in the retina of the eye. The objective is to extract possible spatial relations between them, and to explain their biological implications.

The procedure for obtaining the point patterns used in Sects. 6.1, 6.2 and 6.3 are explained in their respective works [23, 32, 33]. For this paper we have used the point patterns supplied by the authors.

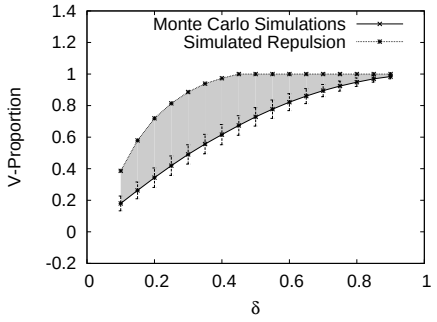

(a) Complete interval

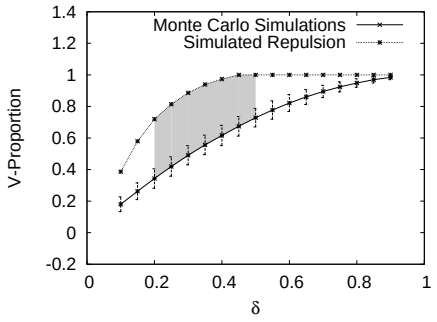

(b) Partial interval

Figure 7: (a) Total area between the V-Proportion curves of the real patterns and the random simulations in Fig. 5. (b) The area corresponding to a subinterval.

In the case of the data points of Sect. 6.4, we manually identified and demarcated the positions of cells on transparent planes from appropriately labeled micrographs or focus planes of overlying retinal layers. This process was carried out using the image processing software ImageJ or Photoshop. The 2d-coordinates of the points in the resulting calibrated mosaics were identified using the ImageJ software. All point patterns can be downloaded from [34].

When calculating the confidence intervals for the Monte Carlo simulations we chose a value of 95% since this is a standard value used in the literature. This value is, however, a free parameter that the user can determine depending on the specific situation in which the experiments are carried out.

Finally, the V-Proportion is based on statistical approximations and its results should be interpreted as the *likelihood* of the existence of a spatial correlation within a certain confidence interval.

6.1. On- and Off-Beta Cells in the Cat Retina

We first study the spatial relations between beta ganglion cells in the retina of a cat (Fig. 8). Beta cells are associated with the resolution of fine detail in the cat's visual system. They can be classified as on- or off-cells, depending on the branching level of their dendritic tree in the inner plexiform layer. Analysis of the spatial pattern provides information on the cat's visual discrimination. In particular, independence of the on- and off-components would strengthen the assumption that there are two separate channels for brightness and darkness [23].

The pattern shown in Fig. 8 was investigated in [23] using histograms of nearest-neighbor distances (ignoring edge effects). To test the independence of the on- and off-patterns, a random translation of the off-component was superimposed on the on-component, and the resulting nearest-neighbor histogram was compared with the original one by a sign reversal test. The authors in [23] concluded that both types of beta cells form a regular lattice, which are superimposed independently. This data was also analyzed in [22] using the J-function with a result greater than 1, which confirmed conclusions in [23]. Our results using the V-proportion are shown in both plots of Fig. 9. Using a confidence interval of 95% we cannot assume any significant spatial relation between on- and off-cells. This result is in accordance with [22] and [23].

6.2. Blue Cones vs Bipolar Cells in the Macaque Retina

The second pair of mosaics we analyze is composed of two different types of neuronal cell populations found in the retina of macaque monkeys: blue bipolar cells and blue cones (Fig. 10). The mosaics used in this study were first presented in [32]. In that work, the authors suggested that blue cones tended to be close to blue bipolar cells and that nearly all blue bipolar cell dendrites terminated beneath the blue cones. The positive correlation of blue cones and blue bipolar cells was confirmed by the same authors in [18] using cross-correlational density recovery profile (cDRP). The finding that the blue cones and the blue bipolar cells were closer together than expected suggests that the position of the perikarya of these neurons were influenced by their synaptic connections or other development interactions [18].

To analyze the mosaics from Fig. 10 we first set the bipolar cells as sites and the blue cones as P points. We then calculated the V-proportion following the approach presented in Sect. 4. As Fig. 11(a) shows, the V-Proportion lies under the simulated one for a band with ranging from 0.2 to 0.6, and within the 95% confidence interval. This result suggets that blue cones tend to be close to blue bipolar cells, and it confirms similar findings in [18]. In a second experiment, we set the blue

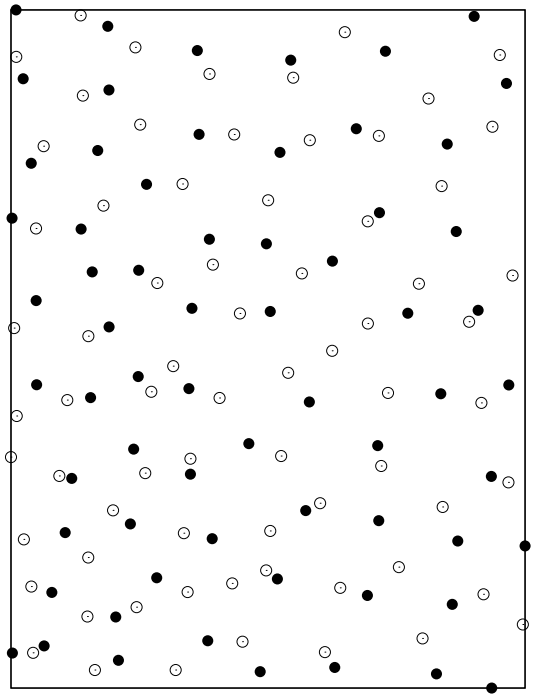

Figure 8: On-cells (filled circles) and off-cells (open circles) from a cat's retina [23].

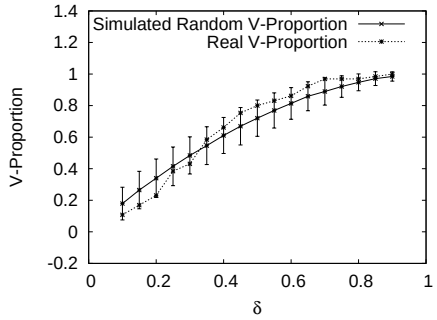

(a) On-cells as sites

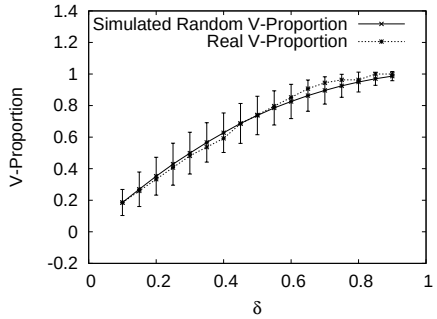

(b) Off-cells as sites

Figure 9: Plots of the V-Proportion of the mosaics from Fig. 8. (a) When the on-cells are used as sites there is no significant spatial relation of off-cells. (b) The lack of spatial patterns between the two populations is even more evident when off-cells are used as sites. Error bars are drawn at the 95% confidence interval.

cones as sites and calculated the V-Proportion of blue bipolar cells. The resulting plot in Fig. 11(b) suggests a positive correlation in this direction as well.

6.3. Short-Wavelength-Sensitive Cones vs Blue Cone Bipolar Cells in the Marmoset Monkey

In a third experiment we analyzed the possible spatial relations between short-wavelength-sensitive (SWS) cones and blue cone bipolar cells in the retina of a marmoset monkey [33]. In this species the S-cone mosaic has an irregular characteristic. In [33], the authors compared the neuronal connectivity of Old World and New World primates, concluding that there exist similarities between them.

In this experiment we first used the blue bipolar cells as sites and analyzed the spatial distribution of the SWS cones. The initial distribution of points is shown in Fig. 12. The V-Proportion of Fig. 13(a) does not show any positive correlation within the 95% confidence interval. However, when swapping the populations (placing SWS as sites), the V-Proportion (Fig. 13(b)) shows a possible positive correlation of blue cone bipolar cells with respect to SWS cells. This last result is in accordance with the behavior of bipolar cells in the Macaque retina shown in Sect. 6.2.

6.4. S-Cone positions vs Irregular Positions among the otherwise hexagonal lattice of M-and L-cones in a Rhesus Macaque Fovea

The foveas of human and primate retinas provide maximum acuity by having highly condensed cone mosaics. Such mosaics had been previously analyzed with respect to lattice regularity [35, 36, 37] but there had been no approach to quantitatively study a possible relationship between S-cone positions and non-hexagonal *defects* of the M/L-cone lattice. In this last experiment we wanted to analyze the spatial relationships of S-cones with a specific feature of foveal microarchitecture.

The analyzed mosaic consists of a minor short wavelength sensitive S-cone and a dominant medium and long wavelength M/L- sensitive cone subpopulation as

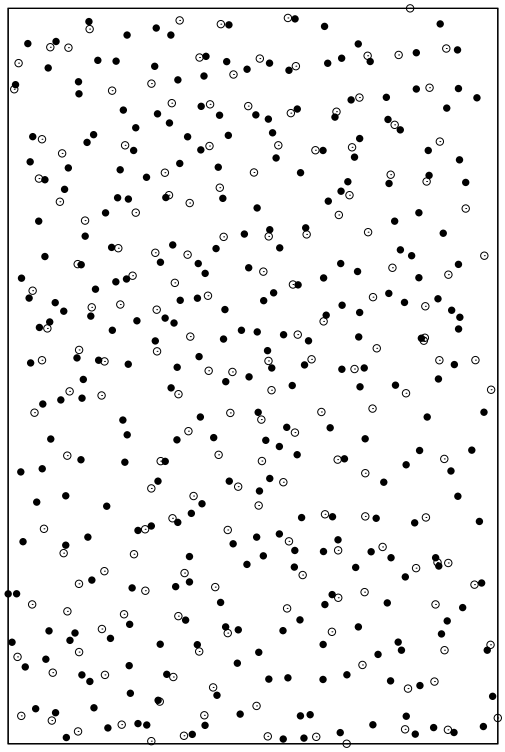

Figure 10: Bipolar cells (filled circles) and blue cones (open circles) from the Macaque retina [32].

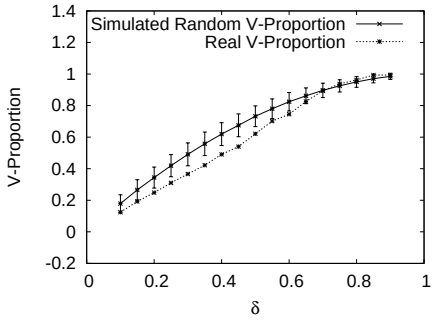

(a) Bipolar cells as sites

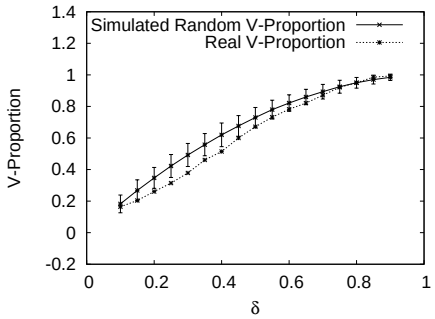

(b) Blue cones as sites

Figure 11: Plots of the V-Proportion of the mosaics from Fig. 10. (a) When the bipolar cells are used as sites, the real V-Proportion lies under the simulated V-proportion and outside its error bars for a band width ranging from 0.2 to 0.6. The error bars of the Monte Carlo simulation are drawn within the 95% confidence interval. This result suggests a positive correlation between blue cones and blue bipolar cells. (b) The V-Proportion plot is calculated when the blue cones are used as sites. This plot also suggests a positive correlation of bipolar cells with respect to blue cones.

shown in Fig. 14. Overall, the foveal mosaic is a highly regular nearly crystalline lattice with predominant 1:6 (hexagonal) neighborship relations. However previous detailed packing analyses [35, 36, 37] have revealed lattice discontinuities represented by cone positions with $< 6 >$ cone neighbors subdividing the hexagonal mosaic in patchy. In a rhesus monkey foveal mosaic with labeled S-cones these positions with irregular number of neighbors have been identified in a previous study [35]. The current approach now allows us to evaluate the S-cone positions in relation to these mosaic distortions.

As revealed in the plot of Fig.15(b) the foveal S-cones tend to be negatively correlated with the irregular positions suggesting that their location is prevalently associated with an undisturbed mosaic zone. This finding has interesting implications for understanding the processes underlying the developmental condensation of this mosaic.

7. Conclusion

This paper presented a method based on the Voronoi diagram to study possible spatial interactions between two cell mosaics. The new measurement, called V-Proportion, is able to detect different types of spatial interdependencies such as positive correlations, negative correlations, as well as lack of correlations. Additionally, the V-Proportion is calculated in a way that a confidence interval can be attached to the resulting behavior eventually revealing the significant range along the relative band widths. Results from simulations as well as in real data sets demonstrate the effectiveness of the V-Proportion method to detect spatial relations between subpopulations of neurons or other (biological) entities.

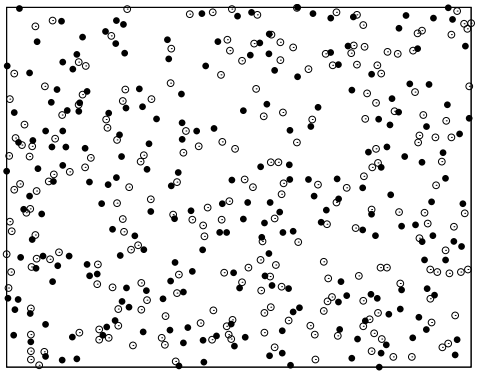

Figure 12: Blue cone bipolar cells (filled circles) and SWS cones (open circles) from a marmoset's retina [33].

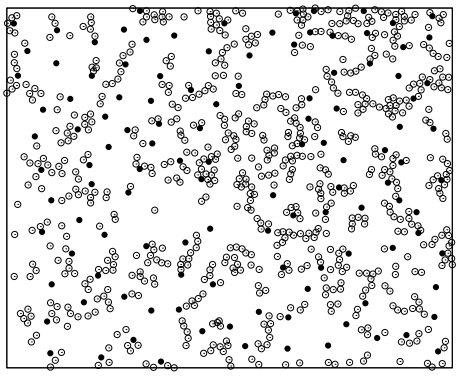

Figure 14: Subpopulation with irregular mosaic positions (< 6 > neighbors) among the otherwise hexagonal lattice of the dominant M/L-cones (open circles) and positions of S-Cones (filled circles) in a rhesus macaque fovea [35].

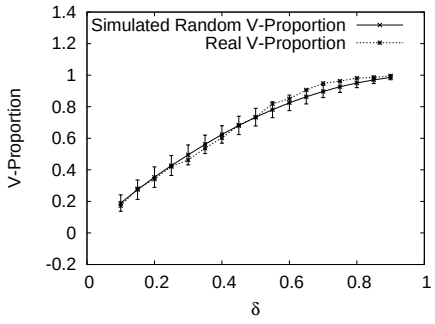

(a) Bipolar cells as sites

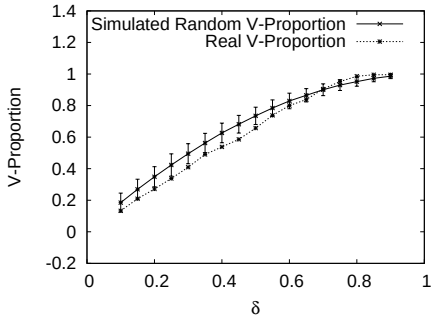

(b) SWS cones as sites

Figure 13: Plots of the V-Proportion of the mosaics from Fig. 12. (a) When the bipolar cells are used as sites the real V-Proportion does not show any significant correlation within the 95% confidence interval. (b) The V-Proportion plot is calculated when the SWS cones are used as sites. This plot suggests a positive correlation of bipolar cells with respect SWS cones within the 95% confidence interval.

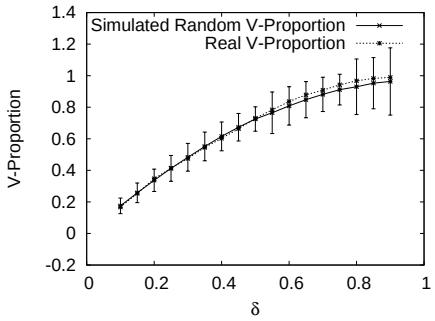

(a) B cones as sites

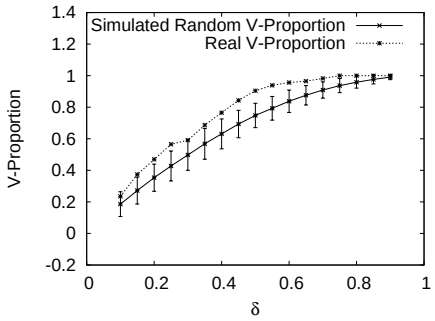

(b) M/L-sensitive cones as sites

Figure 15: V-Proportion plots of the mosaics from Fig 14. (a) When the B cones used as sites, the real V-Proportion does not show any significant correlation within the 95% confidence interval. (b) When the M/L-cones with irregular (non-hexagonal) positions are used as sites, there exist a significant negative correlation within the 95% confidence interval.

Acknowledgments

We want to thank Stephen J. Eglen for making available the beta cells mosaics from [23]. This research has been supported in part by grants SAF2008-303 03694 and CIBER BBN from the Spanish Government and by the Spanish ONCE.

[1] J. Jonas, J. Muller-Bergh, U. Schlotzer-Schrehardt, G. Naumann, Histomorphometry of human optic nerve, Investigative Ophthalmology and Visual Science 31 (1990) 736–744.

[2] H. Kolb, E. Fernandez, R. Nelson, Webvision: the neural organization of the vertebrate retina, http://webvision.med.utah.edu/, 2009.

[3] J. Dowling, The Retina: An Approachable Part of the Brain, Harvard University Press, Cambridge, MA, 1987.

[4] H. Kolb, The neural organization of the human retina, in: J. Heckenlively, G. Arden (Eds.), Principles and Practices of Clinical Electrophysiology of Vision, Mosby Year Book Inc., 1991, pp. 25–52.

[5] C. Morillas, S. Romero, A. Martinez, F. Pelayo, E. Ros, E. Fernandez, A design framework to model retinas, Biosystems 87 (2007) 156–163.

[6] G. J. Chader, J. Weiland, M. S. Humayun, Artificial vision: needs, functioning, and testing of a retinal electronic prosthesis, in: J. Verhaagen, E. M. Hol, I. Huitenga, J. Wijnholds, A. B. Bergen, G. J. Boer, D. F. Swaab (Eds.), Neurotherapy: Progress in Restorative Neuroscience and Neurology, volume 175 of *Progress in Brain Research*, Elsevier, 2009, pp. 317 – 332.

[7] W. Fink, M. Tarbell, CYCLOPS: A mobile robotic platform for testing and validating image processing and autonomous navigation algorithms in support of artificial vision prostheses, Computer Methods and Programs in Biomedicine 96 (2009) 226–233.

[8] A. R. Hafiz, F. Alnajjar, K. Murase, A new dynamic edge detection toward better human-robot interaction, Lecture Notes in Computer Science 5744 (2009) 44–52.

[9] J. Cook, L. Chalupa, Retinal mosaics: new insights into an old concept, Trends in Neuroscience 23 (2000) 26–34.

[10] J. Cook, Spatial regularity among retinal neurons, in: L. Chalupa, J. Werner (Eds.), The Visual Neurosciencies, MIT Press, 2003, pp. 463–477.

[11] P. Ahnelt, H. Kolb, Horizontal cells and cone photoreceptors in primate retina: a Golgi-light microscopic study of spectral connectivity, The Journal of Comparative Neurology 343 (1994) 387–405.

[12] D. Dacey, B. Lee, D. Stafford, J. Pokorny, V. Smith, Horizontal cells of the primate retina: cone specificity without spectral opponency, Science 271 (1996) 656–659.

[13] T. Chan, U. Grünert, Horizontal cell connections with short wavelength-sensitive cones in the retina: a comparison between new world and old world primates, The Journal of Comparative Neurology 393 (1998) 196–209.

[14] P. Ahnelt, E. Fernandez, O. Martinez, J. Bolea, A. Küber-Heiss, Irregular S-cone mosaics in felid retinas. Spatial interaction with axonless horizontal revealed by cross-correlation, Journal of the Optical Society of America A 17 (2000) 580–588.

[15] S. Eglen, Development of regular cellular spacing in the retina: theoretical models, Mathematical Medicine and Biology 23 (2006) 79–99.

[16] E. Fernandez, J. A. Bolea, G. Ortega, E. Louis, Are neurons multifractals?, Journal of Neuroscience Methods 89 (1999) 151–157.

[17] R. Rodieck, The density recovery profile: a method for the analysis of points in the plane applicable to retinal studies, Visual Neuroscience 6 (1991) 95–111.

[18] N. Kouyama, D. Marshak, The topographical relationship between two neuronal mosaics in the short wavelength-sensitive system of the primate retina, Visual Neuroscience 14 (1997) 159–167.

[19] B. Ripley, The second-order analysis of stationary point processes, Journal of Applied Probability 13 (1976) 255–266.

[20] P. Diggle, Displaced amacrine cells in the retina of a rabbit: analysis of a bivariate spatial point pattern, Journal of Neuroscience Methods 18 (1986) 115–125.

[21] M. van Lieshout, A. Baddeley, A nonparametric measure of spatial interaction in point paterns, Statist. Neerdanlica 50 (1996) 344–361.

[22] M. van Lieshout, A. Baddeley, Indices of dependence between types in multivariate point patterns, Scandinavian Journal of Statistics 26 (1999) 511–532.

[23] H. Wässle, B. B. Boycott, R.-B. Illing, Morphology and mosaic of on- and off-beta cells in the cat retina and some functional considerations, Proceedings of the Royal Society of London. Series B (Biological Sciences) 212 (1981) 177–195.

[24] P. Diggle, S. Eglen, J. Troy, Case Studies in Spatial Point Process Modelling, Springer, pp. 215–233.

[25] M. de Berg, O. Cheong, M. van Kreveld, M. Overmars, Computational Geometry: Algorithms and Applications, Springer-Verlag, third edition, 2008.

[26] L. Galli-Resta, E. Novelli, Z. Kryger, G. Jacobs, B. Reese, Modelling the mosaic organization of rod and cone photoreceptors with a minimal-spacing rule, The European Journal of Neuroscience 11 (1999) 1461–1469.

[27] C. Duyckaerts, G. Godefroy, Voronoi tessellation to study the numerical density and the spatial distribution of neurones, Journal of Chemical Neuroanatomy 20 (2000) 83–92.

[28] J. Neyman, E. Scott, A statistical approach to problems of cosmology, Proceedings of the Royal Society of London. Series B (Methodological) 20 (1958) 1–43.

[29] P. Diggle, Statistical analysis of spatial point patterns, Academic Press, 1983.

[30] S. M. Ross, Simulation, Academic Press, 1997.

[31] E. Fernandez, N. Cuenca, J. D. Juan, A compiled basic program for analysis of spatial point patterns: application to retinal studies, Journal of Neuroscience Methods 50 (1993) 1–15.

[32] N. Kouyama, D. Marshak, Bipolar cells specific for blue cones in the macaque retina, Journal of Neuroscience 12 (1992) 1233–1252.

[33] X. Luo, K. K. Ghosh, P. R. Martin, U. Gruenert, Analysis of two types of cone bipolar cells in the retina of a New World monkey, the marmoset, *Callithrix jacchus*, Visual Neuroscience 16 (1999) 707–7191.

[34] `http://www.informatik.uni-freiburg.de/~omartine/mosaics_data_sets.html`, 2010.

[35] D. Pum, P. K. Ahnelt, M. Grasl, Iso-orientation areas in the foveal cone mosaic, Visual Neuroscience 5 (1990) 511–523.

[36] C. Curcio, K. Sloan, Packing geometry of human cone photoreceptors: variation with eccentricity and evidence for local anisotropy, Visual Neuroscience 9 (1992) 169–180.

[37] D. H. Wojtas, B. Wu, P. K. Ahnelt, P. J. Bones, R. Millane, Automated analysis of differential interference contrast microscopy images of the foveal cone mosaic, Journal of the Optical Society of America A, Optics, image science, and vision 25 (2008) 1181–1189.